An Extended Social Force Model via Pedestrian Heterogeneity Affecting the Self-Driven Force

Wenhan Wu, Maoyin Chen, *Member, IEEE*, Jinghai Li, Binglu Liu, and Xiaoping Zheng

***Abstract*— As one of the most effective models for human collective motion, the social force model (SFM) simulates the dynamics of crowd evacuation from a microscopic perspective. However, it treats pedestrians as the homogeneous rigid particles, whereas pedestrians are diverse and heterogeneous in real life. Therefore, this paper develops a pedestrian heterogeneity-based social force model (PHSFM) by introducing physique and mentality coefficients into the SFM to quantify physiology and psychology attributes of pedestrians, respectively. These two coefficients can affect the self-driven force by changing the desired speed, thus characterizing the pedestrian heterogeneity more realistically. Simulation experiments demonstrate that the PHSFM designs a more general and accurate theoretical framework for the expression of pedestrian heterogeneity, which realizes special behavior patterns caused by individual diversity. Furthermore, our model provides effective guidelines for the management of crowds in potential research fields such as transportation, architectural science and safety science.**

***Index Terms*— Crowd dynamics, social force model, pedestrian heterogeneity, evacuation management, nonlinear system.**

I. Introduction

CROWD dynamics have long been a question of great interest in a wide range of fields, which involve human collective behavior in physics [1], traffic flow control in transportation [2], structural design in architectural science [3] and management of large-scale events in safety science [4], etc. The theories and simulation models of crowd dynamics are important, since they play a decisive role in these fields. The existing body of research suggests fascinating impressions of patterns observed in human crowds are adequately rendered by a variety of models [5]. In an attempt to reveal the underlying mechanisms of human crowd motion [6], these models tend to cover physical, biological and social human features, and account for a lot of behavior patterns such as herding behavior [7], self-stopping behavior [8] and group walking behavior [9]. Nevertheless, how to explicate special behavior patterns caused by individual heterogeneity remains a considerable challenge. In fact, a model incorporating heterogeneity could perform more realistic behavior patterns, which has crucial guiding significance for the above-mentioned fields.

From the perspective of modeling, crowd dynamics have been developed following two aspects: macroscopic and microscopic models. Macroscopic models regard the large-scale crowd as fluid or gas from a holistic aspect [10], however, they are inefficient to describe the individual interaction. In contrast, microscopic models are widely applied to uncover the potential laws of crowd motion [11], capturing and elucidating the details of pedestrian movement at the individual level. As one of the most well-known microscopic models, the social force model (SFM) [12], [13], has been successful in simulating the crowd motion and forming self-organization phenomena such as lane formation [12], faster-is-slower effect [13], and stop-and-go waves [14], etc. To our knowledge, however, there are still some problems. Given that the SFM regards pedestrians as the homogeneous rigid particles in Newtonian mechanics, this leads to a practical difficulty in describing individual differences in crowd dynamics. In addition, some influence factors considered by existing improved models are not comprehensive enough, resulting in a lack of versatility [15]. Therefore, incorporating the pedestrian heterogeneity in SFM is significant and challenging.

On the one hand, pedestrians are deemed to be average soccer fans, whose shape, mass and desired speed are nearly assumed to be homogeneous [9], [13]. Although this assumption simplifies the complexity of SFM to some extent, it is contrary to actual situations because pedestrians in crowds are diverse and heterogeneous. In recent researches, Song *et al.* [16] considered the multi-circle model can more realistically represent the two-dimensional body shape of pedestrians. Moussaïd *et al.* [17] adopted heuristics rules to simulate collective social behaviors according to the difference of vision range. From the individual point of view, the above characteristics are unique pedestrian attributes (i.e. age, gender, height, weight, body shape, and vision range, etc.), which are called as physiology attributes in this paper. However, taking the physiology attributes into account may raise some theoretical issues. Older people tend to adopt a more conservative basic gait pattern [18], but do young people have advantages over elders in the movement process? How does the relationship between height and weight affects evacuation efficiency? The potential answers to the above questions may be very interesting.

Manuscript received 14 June 2020; revised 8 February 2021; accepted 17 April 2021. Date of publication 5 May 2021; date of current version 8 July 2022. This work was supported in part by the National Key Research and Development Program of China under Grant 2020YFF0304900, in part by the National Major Scientific Research Instrument Development Project under Grant 61927804, and in part by the National Natural Science Foundation of China under Grant 61773233. The Associate Editor for this article was Z. Duric. *(Corresponding author: Xiaoping Zheng.)*

The authors are with the Department of Automation, Tsinghua University, Beijing 100084, China (e-mail: wwh19@mails.tsinghua.edu.cn; mychen@mail.tsinghua.edu.cn; ljhai725@163.com; liubl17@mails.tsinghua.edu.cn; asean@mail.tsinghua.edu.cn).

Digital Object Identifier 10.1109/TITS.2021.3074914

On the other hand, when an emergency or disaster occurs, pedestrians may perform irrational behaviors due to the change of psychological state. The SFM can simulate the dynamic characteristics of escape panic, while the factors influencing pedestrian psychology are multiple in realistic scenarios. To measure the heterogeneity at the psychological level, psychology attributes (i.e. identity, character, temperament, and familiarity, etc.) are illustrated to describe the dynamic perception of environmental change. Social psychologists proposed the theories of cognitive behavior, social identity, and cooperation and competition [19], [20], which characterize the impact of different psychology attributes on pedestrians in realistic scenes. Nevertheless, most of these theories are conceptual descriptions, lacking sufficient mathematical expression and model support [21].

In recent years, existing researches have recognized the critical role played by pedestrian heterogeneity in crowd simulations. For discrete models, they were mainly characterized by heterogeneous updating rules. Guo *et al.* [22] established a heterogeneous lattice gas model considering the critical damage force, local density, and exit congestion. Li *et al.* [23] proposed a behavior-based cellular automata model to express the motion feature and behavior preference of diverse pedestrians. With regard to continuous models, studies conducted by relevant researchers [24]–[26] have shown that factors such as cognitive capability, physical strength degree, and types of disabled people could be included in SFM to reflect the pedestrian heterogeneity, making the simulation more realistic. However, these models are difficult to form a general framework, resulting in poor scalability when other heterogeneous clues are considered. Moreover, there existing certain limitations in crowd simulation software when it comes to pedestrian heterogeneity [27]. Although Legion and STEPS are based on cellular automata model and possess high computational efficiency, they lack the ability of secondary development to incorporate heterogeneous factors. AnyLogic and PTV Viswalk, supported by SFM as modeling principle, are reliable tools for simulating crowd dynamics. Whereas it is still an open question to embed pedestrian heterogeneity into the above software as a universal extension component, especially comprising physiology and psychology features.

To establish a more general and accurate theoretical framework from the perspective of physiology and psychology attributes, this paper proposes a pedestrian heterogeneity-based social force model (PHSFM), which effectively overcomes the above problems. The physique and mentality coefficients are simultaneously employed to quantify pedestrian heterogeneity, which affects the desired speed in SFM. In fact, the simplicial representations are indeed more suited than merely one or several factors involving the heterogeneity to describe the human crowds in real-world situations. From the experiments based on library simulation scenarios, we demonstrate the PHSFM simulates the pedestrian evacuation process more realistically in response to different emergencies. The comparative analysis with existing improved models illustrates how the PHSFM describes the pedestrian heterogeneity in a more general way. Furthermore, both additive and multiplicative rules provide a direction for more comprehensive interpretations of pedestrian heterogeneity.

The rest of this paper is organized as follows. In Section II, physique and mentality coefficients are quantified, and the PHSFM is illustrated. Section III provides corresponding numerical simulations and analyzes the effect of pedestrian heterogeneity on crowd evacuation. Finally, the discussion and future research topics are described in Section IV.

II. Model

A. Physique Coefficient

The physiology attributes of pedestrian i at time t are represented by a function $P_i(t)$, which represents the physique coefficient. Physiology attributes are characterized by high stability with slight variation, where the stability refers to the sensitivity of pedestrians to internal perturbations caused by muscles or neural control [28]. On the one hand, owing to the instinctual reflex of pedestrians on emergencies, the dynamic process of physiology attributes is considered to be a fluctuation response confined to a specific range [29], approximated by one-dimensional Brownian motion. On the other hand, the risk index $\lambda \in [0, 1]$, used to measure the degree of emergencies, has a certain impact on the volatility of physique coefficient. Thus, for $\forall t \geq t_0$, $\Delta t > 0$, the physique coefficient $P_i(t)$ can be expressed as follows:

$$P_i(t + \Delta t) - P_i(t) \sim \mathcal{N}\left(0, \lambda^2 \Delta t\right) \tag{1}$$

where $\mathcal{N}(\cdot)$ denotes the normal distribution and the time step is set to $\Delta t = 0.04s$, $P_i(t)$ is a continuous function of t with stationary independent increment. Compared with the Gaussian distribution, the Beta distribution limits the value interval and has the parameter flexibility, it is more reasonable to assign physique coefficients for different types of pedestrians at initial time t_0. Assuming a random variable $X_i \sim Beta(\alpha, \beta)$, and the corresponding probability density function is given by:

$$f_{X_i}(x_i | \alpha, \beta) = \frac{\Gamma(\alpha + \beta)}{\Gamma(\alpha)\Gamma(\beta)} x_i^{\alpha-1}(1 - x_i)^{\beta-1} \tag{2}$$

where $\alpha > 0$, $\beta > 0$, and $\Gamma(\cdot)$ represents the Gamma function. The random variable X_i is transformed as the location-scale family, constructing a mapping function $g : \mathcal{D} \to \mathcal{R}$ on the interval $\mathcal{D} = [0, 1]$. Then the physique coefficient of pedestrian i at initial time t_0 can be obtained in the following form:

$$g(\mathrm{D}) = \{P_i(t_0) | P_i(t_0) = \mu + \sigma x_i, x_i \in \mathcal{D}\} \tag{3}$$

Here, the location parameter $\mu \in \mathcal{R}_+$ and the scale parameter $\sigma \in \mathcal{R}_+$ determine the lower bound and the interval range of $P_i(t_0)$, respectively.

In this case, the range of $P_i(t)$ is evaluated according to the empirical data of stride interval time series in gait dynamics theory [30]. The fluctuation interval is given by:

$$P_i(t) \in [(1 - \Delta_P) P_i(t_0), (1 + \Delta_P) P_i(t_0)] \tag{4}$$

in which Δ_P denotes the maximum fluctuation range, with a general approximation of $\Delta_P \approx 0.1$.

B. Mentality Coefficient

From the psychological perspective, the SFM fails to effectively reveal the pedestrian heterogeneity, since the psychology characteristics are complicated during the evacuation process. Therefore, we employ the mentality coefficient to describe the comprehensive psychology states of pedestrians in real scenes.

Social psychology studies show that "stress" is a more accurate concept than "panic" to describe the pedestrian psychology [31]. The stress of a pedestrian originates from the cognition to other individuals and environments. Although the panic parameter $p_i(t) = 1 - \bar{v}_i(t)/v_i^0$ is proposed to measure the impatience of pedestrians [13], it ignores the influence of environments. However, the degree of emergencies is confirmed to make the psychology attributes of pedestrians differ from that in normal conditions [31].

Hence, the impact of emergencies on psychology can be considered as another factor, which is assumed as an exponential function of the risk index λ. Summing up the above illustration, the stress of pedestrian i is defined as follows:

$$s_i(t) = \exp(\lambda)\left\{[1 - p_i(t)]\,\delta_i^{nor} + p_i(t)\,\delta_i^{\max}\right\} \tag{5}$$

Here, $\delta_i^{nor} = v_i^{nor}/v_i^0$ and $\delta_i^{\max} = v_i^{\max}/v_i^0$, where v_i^{nor} is the desired speed in normal and $v_i^{\max}$ the maximum desired speed in panic. Generally, the value of δ_i^{nor} is equal to 1.

Further, the discomfort can be felt by pedestrian i if other individuals appear in his/her personal zone (0.46–1.22m) [32], which can be represented by a circular area with a radius $\tilde{r}_i \approx 4r_i$. The pedestrian density in the personal zone can be expressed by the following:

$$\rho_i(t) = n_i(t)/\pi\tilde{r}_i^2 \tag{6}$$

where $n_i(t)$ denotes the number of pedestrians in this zone at time t. As the pedestrian density increases, the stimulus intensity signals of surrounding environment are simultaneously relayed to the mechanism of enhancement and suppression [33], which may inspire two other interesting psychology states, namely cooperation and competition.

The current researches on evacuation dynamics [34] indicate that the cooperation frequency can be maintained at a high level when the risk index is low. As the risk index raises, the cooperation frequency decreases. However, there may still exist cooperative behavior even if the emergency is life-threatening. Based on the above analysis, the probability of cooperation in the personal zone is assumed to follow a Boltzmann-like relation with the risk index λ:

$$\gamma_i(\lambda) = \gamma_0 \exp(-w_i\lambda) \tag{7}$$

Here, $\gamma_0 = 0.95$ represents the cooperation probability in non-emergency evacuation scenario and w_i is the attenuation rate of the cooperation probability, inseparable from the social psychology and subjective cognition of pedestrian i. Assuming the random variable η_i of psychological state selection follows the Bernoulli distribution, expressed as follows:

$$\eta_i = \begin{cases} +1, & 1 - \gamma_i(\lambda) \\ -1, & \gamma_i(\lambda) \end{cases} \tag{8}$$

Here, $\eta_i = -1$ if pedestrian i chooses to cooperate, otherwise $\eta_i = +1$ corresponds to pedestrian i competes with others.

In order to acquire the expression of mentality coefficient, the Sigmoid function is also introduced to quantify the state transition process, similar to the neuron activation response [35]. The function of state transition is written as follows:

$$\psi_i(t) = \frac{1}{1 + \exp\left[-\eta_i\rho_i(t)/k_M\right]} \tag{9}$$

where k_M indicates its slope. If the stress is regarded as a basic state, the transition of psychology state occurs when the pedestrian density in the personal zone changes. Thus, the mentality coefficient of pedestrian i can be described by:

$$M_i(t) = s_i(t)\left[(1 - \Delta_M) + 2\Delta_M\psi_i(t)\right] \tag{10}$$

where Δ_M is the maximum mutation. In the simulation, $\Delta_M \approx 0.5$ according to the reaction performance of the neurocognitive mechanism.

C. Pedestrian Heterogeneity-Based Social Force Model

The SFM is based on Newtonian mechanics to simulate crowd motion. However, many expansions of SFM [17], [36] including itself treat pedestrians as the same particles, which has certain limitations. Therefore, the PHSFM is developed from the physiology and psychology levels. The combined effect of forces leads to dynamic changes in pedestrian acceleration, which is based on the nonlinear coupled Langevin equations of motion:

$$m_i\frac{d\mathbf{v}_i(t)}{dt} = \mathbf{f}_{id}^H + \sum_{j(\neq i)}\mathbf{f}_{ij} + \sum_W \mathbf{f}_{iW} \tag{11}$$

where $\mathbf{f}_{id}^H$, $\mathbf{f}_{ij}$ and $\mathbf{f}_{iW}$ respectively represent a self-driven force generated by the pedestrian, a force on the pedestrian due to agent-neighbor interactions, and an interaction force between the pedestrian and the walls. Note that the self-driven force with pedestrian heterogeneity is neglected by SFM.

Here, the self-driven force $\mathbf{f}_{id}^H$ with pedestrian heterogeneity is established by the following:

$$\mathbf{f}_{id}^H = m_i\frac{H_i(t)\,v_i^0\mathbf{e}_i^0 - \mathbf{v}_i(t)}{\tau_i} \tag{12}$$

in which the heterogeneous coefficient $H_i(t) = P_i(t) \circ M_i(t)$ is composed of a functional relationship $\circ$ between physique and mentality coefficients. Besides, pedestrian i of mass m_i tends to move with the initial desired speed v_i^0 and desired direction $\mathbf{e}_i^0$, and τ_i is related to a certain relaxation time for pedestrian i to adapt to the actual speed.

The interaction force $\mathbf{f}_{ij}$ between pedestrian i and j is borrowed from the SFM:

$$\begin{aligned}\mathbf{f}_{ij} = {} & A_i\exp\left[(r_{ij} - d_{ij})/B_i\right]\mathbf{n}_{ij} + kg\left(r_{ij} - d_{ij}\right)\mathbf{n}_{ij} \\ & + \kappa g\left(r_{ij} - d_{ij}\right)\Delta v_{ji}^t\mathbf{t}_{ij}\end{aligned} \tag{13}$$

where $A_i\exp\left[(r_{ij} - d_{ij})/B_i\right]\mathbf{n}_{ij}$, $kg\left(r_{ij} - d_{ij}\right)\mathbf{n}_{ij}$, and $\kappa g\left(r_{ij} - d_{ij}\right)\Delta v_{ji}^t\mathbf{t}_{ij}$ correspond to the repulsive interaction force, body force, and sliding friction force from pedestrian i to j, respectively. A_i and B_i are constants, r_{ij} and d_{ij}

TABLE I
SETTING OF PARTIAL PARAMETERS IN PHSFM

Symbol	Description	Value
m_i	Pedestrian mass	$80\ kg$
v_i^0	Initial desired speed	$1\ ms^{-1}$
τ_i	Relaxation time	$0.5\ s$
A_i	Constant 1	$2 \cdot 10^3\ N$
B_i	Constant 2	$0.08\ m$
r_i	Pedestrian radius	$0.25 \sim 0.35\ m$
k	Body elasticity coefficient	$1.2 \cdot 10^5\ kgs^{-2}$
κ	Sliding friction coefficient	$2.4 \cdot 10^5\ kgm^{-1}s^{-1}$

denote the radius sum and the distance between the centroids of pedestrian i and j, and $\mathbf{n}_{ij}$ represents the normalized vector pointing from pedestrian j to i. Besides, k and κ are both constants, which refer to body elasticity coefficient and sliding friction coefficient. $\mathbf{t}_{ij}$ is the tangential direction and $\Delta v_{ji}^t = \left(\mathbf{v}_j - \mathbf{v}_i\right) \cdot \mathbf{t}_{ij}$ holds the tangential speed difference. When two pedestrians have no physical contact ($r_{ij} < d_{ij}$), $g(x)$ is zero; otherwise, it equals to x.

The last force $\mathbf{f}_{iW}$ is generated by the interaction between pedestrian i and the walls, similar to the expression of $\mathbf{f}_{ij}$:

$$\mathbf{f}_{iW} = A_i \exp\left[\left(r_i - d_{iW}\right)\big/ B_i\right]\mathbf{n}_{iW} + kg\left(r_i - d_{iW}\right)\mathbf{n}_{iW} - \kappa g\left(r_i - d_{iW}\right)\left(\mathbf{v}_i \cdot \mathbf{t}_{iW}\right)\mathbf{t}_{iW} \quad (14)$$

where $A_i \exp\left[\left(r_i - d_{iW}\right)\big/ B_i\right]\mathbf{n}_{iW}$, $kg\left(r_i - d_{iW}\right)\mathbf{n}_{iW}$, and $\kappa g\left(r_i - d_{iW}\right)\left(\mathbf{v}_i \cdot \mathbf{t}_{iW}\right)\mathbf{t}_{iW}$ represents the repulsive interaction force, body force, and sliding friction force from pedestrian i to wall W. Here, d_{iW} is the distance between the center of pedestrians i and the surface of wall W, $\mathbf{n}_{iW}$ represents the normalized vector perpendicular to it, and $\mathbf{t}_{iW}$ denotes the tangential direction.

The PHSFM affects the desired speed in SFM by incorporating the pedestrian heterogeneity, while the parameters of other terms in PHSFM are consistent with that in SFM. Following the reasonable assumptions in [13], partial parameters and corresponding values involved in PHSFM are summarized in Table I. Furthermore, Fig. 1 illustrates the flowchart of the simulation process by PHSFM.

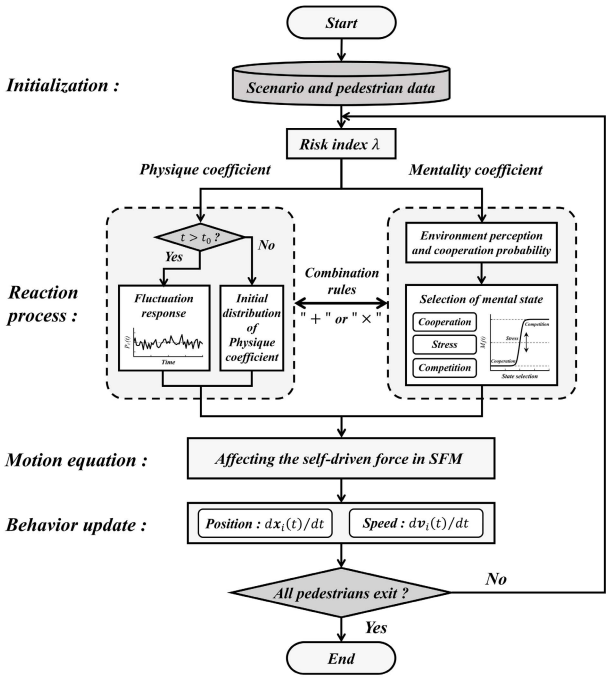

Fig. 1. Flowchart of the simulation process by PHSFM.

III. NUMERICAL SIMULATIONS

A. Experiment Setup

An empirical survey was conducted in Humanities and Social Sciences Library of Tsinghua University in 2020, and all participants were guaranteed to receive the survey without being informed in advance. The purpose of our survey was to obtain the proportion of different types of pedestrians in the library scene. Through random sampling, we discovered that 157 participants (1/5 of the population size) consisted of 108 college students (proportion = 68.79%; age = 22.41 ± 3.78 yr (mean ± s.d.); 59 males, 49 females), 29 professors (proportion = 18.47%; age = 52.67 ± 9.83 yr (mean ± s.d.); 18 males, 11 females), 14 library staff (proportion = 8.92%; age = 38.13 ± 5.48 yr (mean ± s.d.); 5 males, 9 females) and 6 other people (proportion = 3.82%; age = 41.05 ± 4.75 yr (mean ± s.d.); 3 males, 3 females). The proportions of students, professors and staff are approximately 70%, 20% and 10%, regardless of the random influence of other people. In the simulation experiment, the parameters are set according to the above-mentioned proportions and survey data.

In this paper, we try to simulate the crowd evacuation in a library scene. After inspecting the actual layout of each scene in the library, the following two common scenes are selected for our simulation. One is the main corridor of 40 m length and 5 m width in the library. The pedestrians gather from other rooms to one side of the corridor and escape towards the exit of 2 m width on the other side. Another is the reading room of 24 m length and 16 m width with a 2 m wide single exit. In case of emergency, the whole pedestrians randomly distributed in the reading room escape towards the exit. The simulation experiment is carried out by equally scaling the scene and pedestrians for the above two scenes.

In order to simulate the evacuation for unsuspected incidents, we use the risk index $\lambda \in [0, 1]$ to measure the degree of emergencies. According to the types (i.e. fire, terrorist attack, etc.) and the scales (i.e. slight, severe, etc.) of incidents, the degree of emergencies is divided into three levels, namely $\lambda \in [0, 0.3)$, $\lambda \in [0.3, 0.7]$, $\lambda \in (0.7, 1.0]$, which respectively represent mild level ($*$), moderate level ($**$), and severe level ($***$). Note that the risk index λ grows up with the increase in the degree of emergencies.

B. Effect of Physique Coefficient on Crowd Evacuation

In general, although the physique characteristics for specific crowd are generated by the Gaussian distribution [37], the values such as negative numbers and outliers in Gaussian distribution may have no practical meaning. For simplicity, we set $\alpha = \beta \geq 1$ in Beta distribution to obtain the

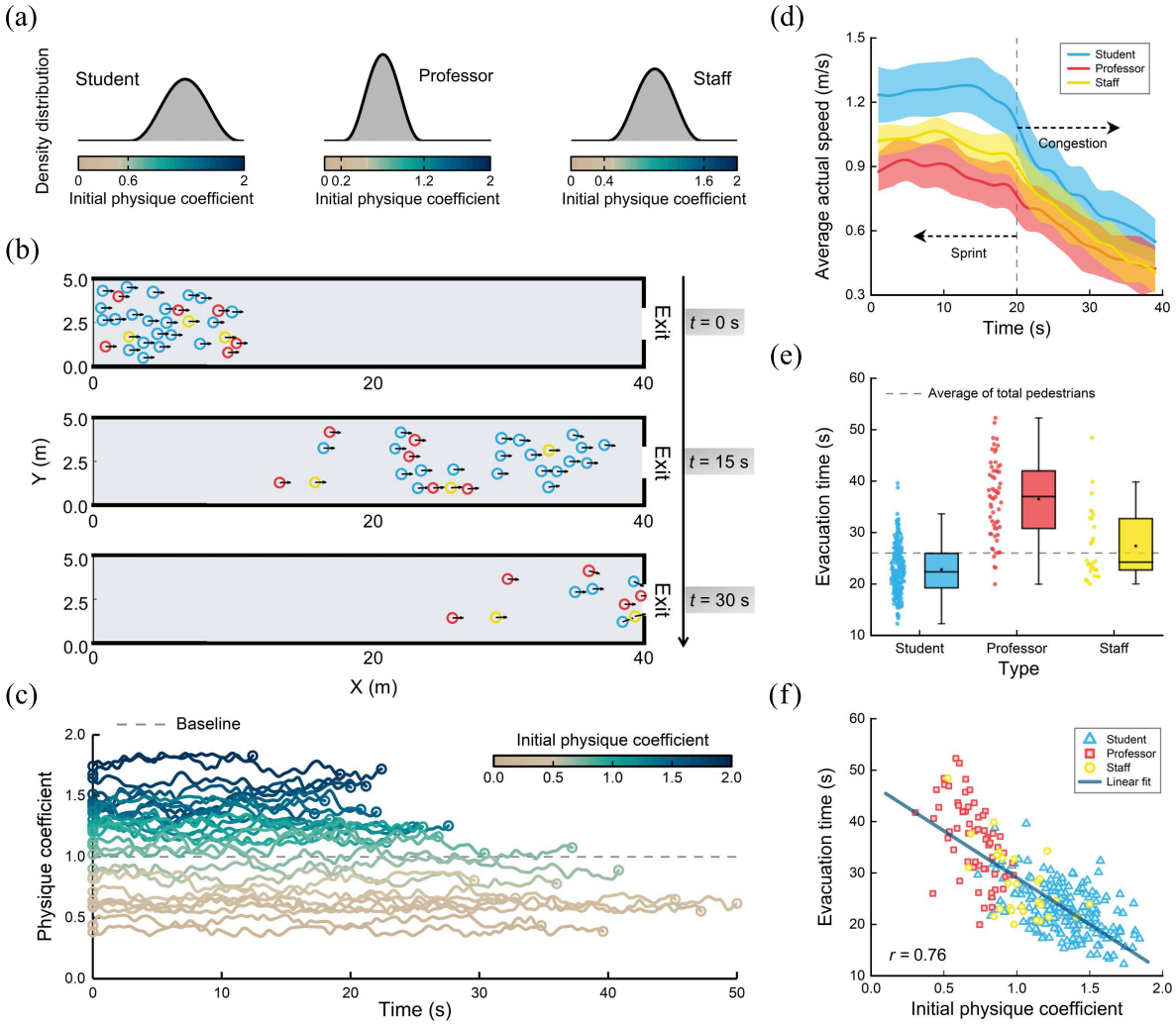

Fig. 2. Effect of physique coefficient on crowd evacuation. (a) Distributions of physique coefficients for specific crowd. (b) Snapshots of crowd evacuation under the effect of physique coefficient in the main corridor at 0s, 15s and 30s. The blue, red and yellow circles represent students, professors and staff, respectively. (c) Effect of the initial physique coefficient of pedestrians, as shown by the temporal evolution of the physique coefficient during the evacuation process. The curves with different colors correspond to different values for the initial physique coefficients of pedestrians. The dashed horizontal line is a baseline corresponds to the SFM. (d) Time-varying trend of the average actual speed for specific crowd. The solid lines and error bands respectively represent the mean and standard deviation in 10 trials. (e) Box plot of evacuation time for specific crowd. The points represent the simulation data in 10 trials, and the dotted line denotes the average of total pedestrians. (f) High correlation ($r = 0.76$) between the evacuation time and the initial physique coefficient suggests physiology attributes are crucial features that determine the evacuation time. The shape points correspond to the simulation data in 10 trials.

"approximate Gaussian distribution" within a limited interval. Note that the values of α and β can also be adjusted to distinguish different crowds. In the experiment, the physique coefficients of students, professors and staff are assumed to be relatively strong, weak and medium, the initial distributions of which are shown in Fig. 2(a), corresponding to three different intervals.

Due to the structure of the library corridor, pedestrians are less affected by the initial location and congestion, thus it is beneficial to test the model based on physiology heterogeneity. Supposing that the risk index $\lambda = 0.5$ and 30 pedestrians scatter on one side of the corridor (21 students, 6 professors and 3 staff). The snapshots depict the crowd escaped from one side to the other of the corridor in Fig. 2(b), the simulation phenomenon agrees well with the empirical observation. Students with strong physique coefficients appear to "catch up" ($t = 15\ s$) while professors with weak physique coefficients show "fall behind" ($t = 30\ s$), which intuitively explains the heterogeneous influence of physiology attributes. The temporal dynamics of physique coefficients are illustrated in Fig. 2(c), where various curves show how the physique coefficients of pedestrians evolve when initial values of different sizes are considered. Notably, the fluctuation of physique coefficient is relatively stable, with a larger physique coefficient corresponds to a wider range of fluctuation. The termination time depends on the initial value of physique coefficient, implying the existence of a certain connection between the physique coefficient and evacuation time.

To quantitatively analyze the influence of physique coefficient on specific crowd, the average actual speed of crowd Ω at

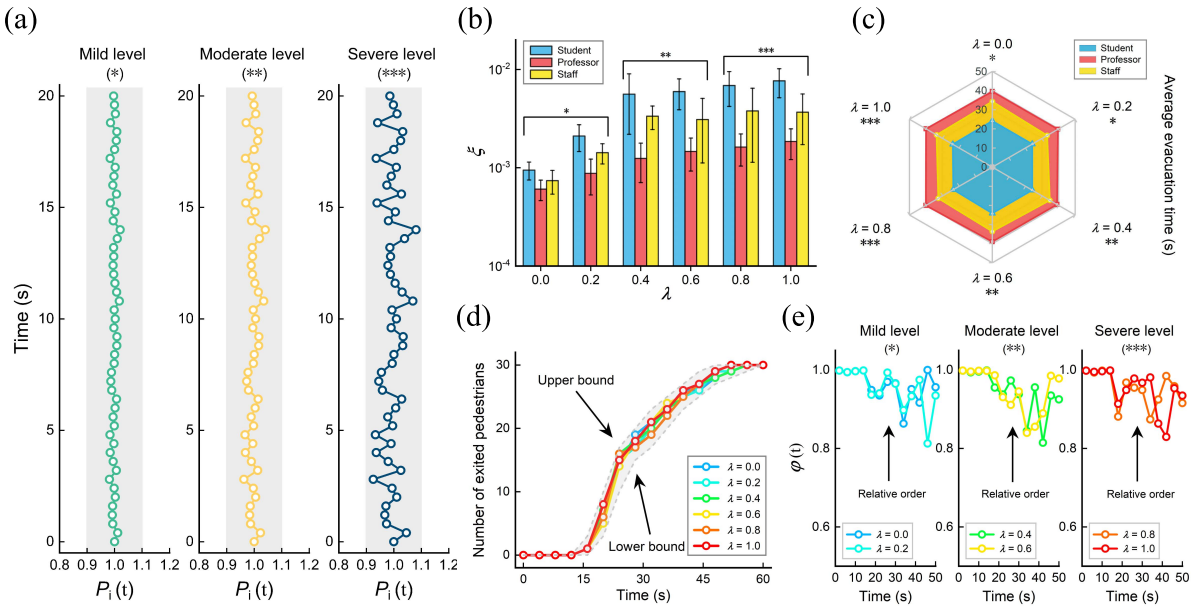

Fig. 3. Influence of risk index on physiology attributes. (a) Fluctuation dynamics of physique coefficient under mild, moderate and severe levels, a higher risk index corresponds to a more violent fluctuation in the fixed interval. (b) Variations of the standard deviation of fluctuation for specific crowd under different risk indexes. (c) Radar map of the average evacuation time for specific crowd under different risk indexes. (d) Temporal dynamics of the number of exited pedestrians under the influence of risk index. The gray dotted lines correspond to the upper and lower bounds and the gray area is the fluctuation interval. (e) Variations of the order parameter under mild, moderate and severe levels. High order parameters demonstrate the crowd holds relatively order regardless of the risk index.

time t is defined as follows:

$$\bar{v}_\Omega(t) = \frac{1}{N_\Omega} \sum_{i \in \Omega} |\mathbf{v}_i(t)| \tag{15}$$

where Ω represents the specific crowd and N_Ω is the number of pedestrians in crowd Ω. In Fig. 2(d), there are obvious differences between the average actual speed among students, professors and staff regardless of the sprint phase or the congestion phase, which is consistent with the phenomenon that emerged in Fig. 2(b). Naturally, the box plot of Fig. 2(e) indicates that students with superior physiology attributes occupy a dominant position in the process, whereas the evacuation efficiencies of staff and professors decrease in turn. Moreover, as shown in Fig. 2(f), the evacuation time and the initial physique coefficient are found to have a high correlation $r = 0.76$ even if there are interferences caused by locations and obstructions, which validates the inference from Fig. 2(c). Thus, it is preliminarily illustrated that our model achieves a more consistent phenomenon with the empirical observation by incorporating the physiology heterogeneity.

C. Influence of Risk Index on Physiology Attributes

In addition, we want to know whether the risk index λ affects the above simulation results. Fig. 3(a) presents the fluctuation dynamics of physique coefficient under different risk degrees. We take the pedestrian i with $P_i(t_0) = 1$ as an example, it is clear that a higher risk index corresponds to a more violent fluctuation in the fixed interval [0.9, 1.1]. Assuming that t_i is the exited moment of pedestrian i, the standard deviation of fluctuation ξ_i is defined for quantitative analysis and can be calculated as follows:

$$\xi_i = \sqrt{\frac{1}{t_i - t_0} \sum_{t=t_0}^{t_i} [P_i(t) - P_i(t_0)]^2} \tag{16}$$

As shown in Fig. 3(b), in the horizontal direction, the standard deviation of fluctuation grows up as the risk index λ increases. In the vertical direction, when the risk index λ is fixed, there are differences in the standard deviation of fluctuation among various crowds. This reflects the impact of risk index λ on physiology attributes for different types of pedestrians. However, the average evacuation time corresponds to specific crowd is almost maintained at a stable state in Fig. 3(c), which demonstrates the physiology attributes still hold high stability regardless of the degree of fluctuation.

When all pedestrians are viewed as a whole, the curves of evacuation efficiency are depicted in Fig. 3(d). The upper and lower bounds of evacuation efficiency represent the situation where the physique coefficient is taken as two critical values of the fluctuation interval. Even if the risk index varies, the evacuation efficiency of pedestrians is still limited to the fluctuation interval. To explore the internal laws of crowd dynamics at each moment, a system order parameter proposed by Vicsek *et al.* [38] is adopted to measure the order of pedestrian motion. The order parameter is defined as follows:

$$\varphi(t) = \frac{1}{\sum_{i=1}^{N} |\mathbf{v}_i(t)|} \left| \sum_{i=1}^{N} \mathbf{v}_i(t) \right| \tag{17}$$

where N is the number of remaining pedestrians. As expected from the results in Fig. 3(e), the order parameters are

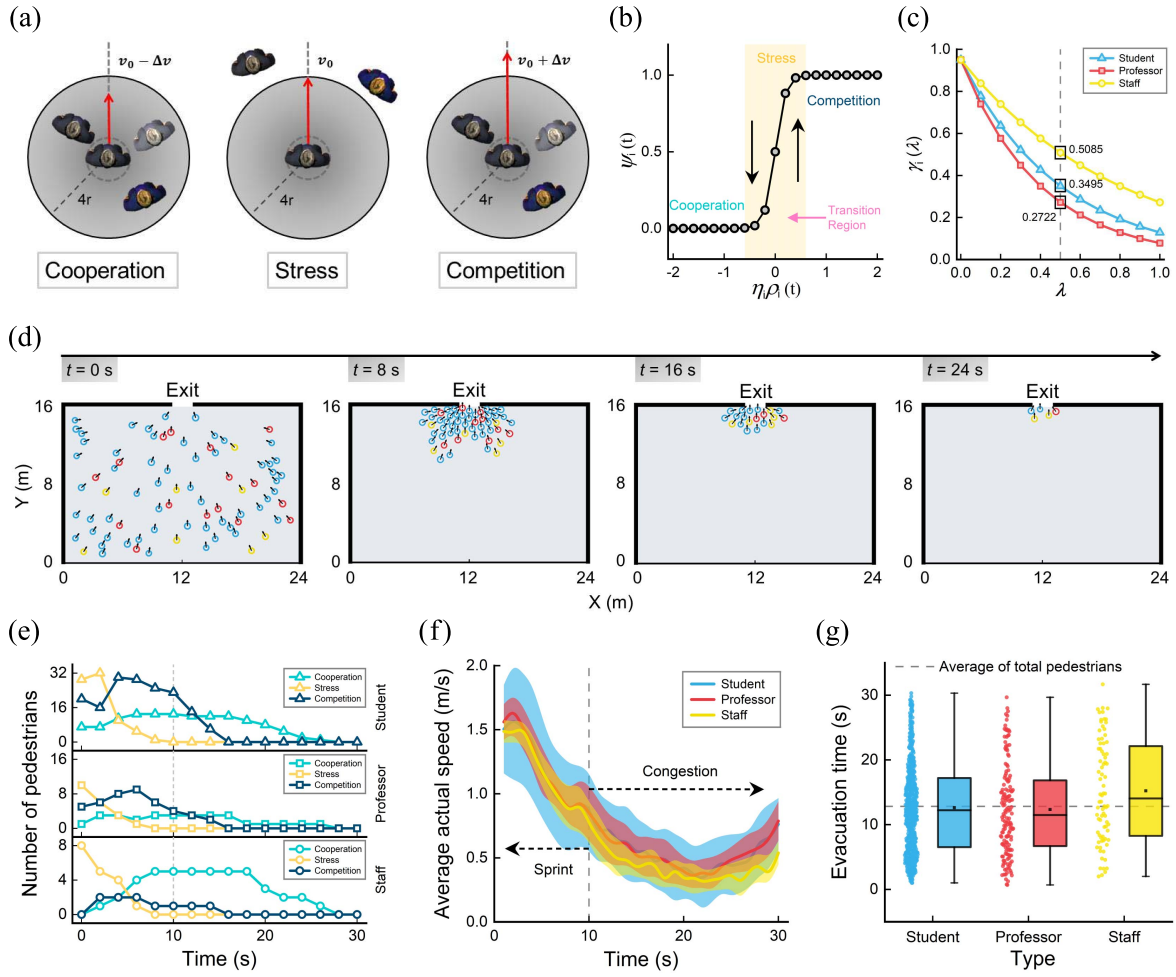

Fig. 4. Effect of mentality coefficient on crowd evacuation. (a) Three kinds of psychology states available to each pedestrian. Given that its previous moving direction is along the dashed line, where cooperation, stress and competition respectively correspond to slow, normal and fast movements in the same direction. (b) Transition process of different psychology states, the positive direction is activated as a competitive state while the negative direction is a cooperative state. (c) Cooperation probability as a function of the risk index, the attenuation rates of staff, students and professors increase in turn. (d) Snapshots of crowd evacuation under the effect of mentality coefficient in the reading room at 0s, 8s, 16s and 24s. The blue, red and yellow circles represent students, professors and staff, respectively. (e) Temporal evolution of the number of pedestrians in different psychology states. All states exist on the left side of the dashed line, while only cooperation and competition exist on the right side due to the crowd aggregation. (f) Time-varying trend of the average actual speed for specific crowd. The solid lines and error bands respectively represent the mean and standard deviation in 10 trials. (g) Box plot of evacuation time for specific crowd. The points represent the simulation data in 10 trials, and the dotted line denotes the average of total pedestrians.

significantly high under mild, moderate and severe levels. The crowd holds relatively order under different risk indexes, further indicating the high stability of physiology attributes.

D. Effect of Mentality Coefficient on Crowd Evacuation

The threat perception is closely related to pedestrian psychology, leading to differences in personal decision-making. Accordingly, it is worth discussing the effect of mentality coefficient on the evacuation process by neglecting the physiology attributes. The pedestrian is in a state of stress if no individual appears in the personal zone, and the state of stress may be transformed into a state of either cooperation or competition when other individuals emerge in the area. These three potential psychology states are described in Fig. 4(a), resulting in the decrease, maintenance and increase of the desired speed. Fig. 4(b) shows the transition process of three kinds of psychology states, where the activation of Sigmoid function is related to cooperation probability η_i and pedestrian density $\rho_i\,(t)$. Note that the stress is activated as a competitive state in the positive direction while the negative direction is a cooperative state.

Sociological studies pointed out that pedestrians in different social groups possess characteristic behavior mechanisms, caused by the interaction of psychological perception and social assessment process [39]. Hence, students, professors and staff show different cooperation probabilities in the face of an emergency. The cooperation probability of staff is relatively high, since it is their responsibility to assist students and professors to evacuate. Considering the social status of professors, their cooperation probability may be slightly lower than that of students. Thereby, for students, professors and staff, the attenuation rate of cooperation probability is simply assumed to be $\omega_i = 2.0, 2.5$ and 1.25. Fig. 4(c) presents the cooperation probability $\gamma_i\,(\lambda)$ as a function of the risk index λ, there existing a distinct difference in cooperation probability among various crowds when the risk index is fixed as $\lambda = 0.5$.

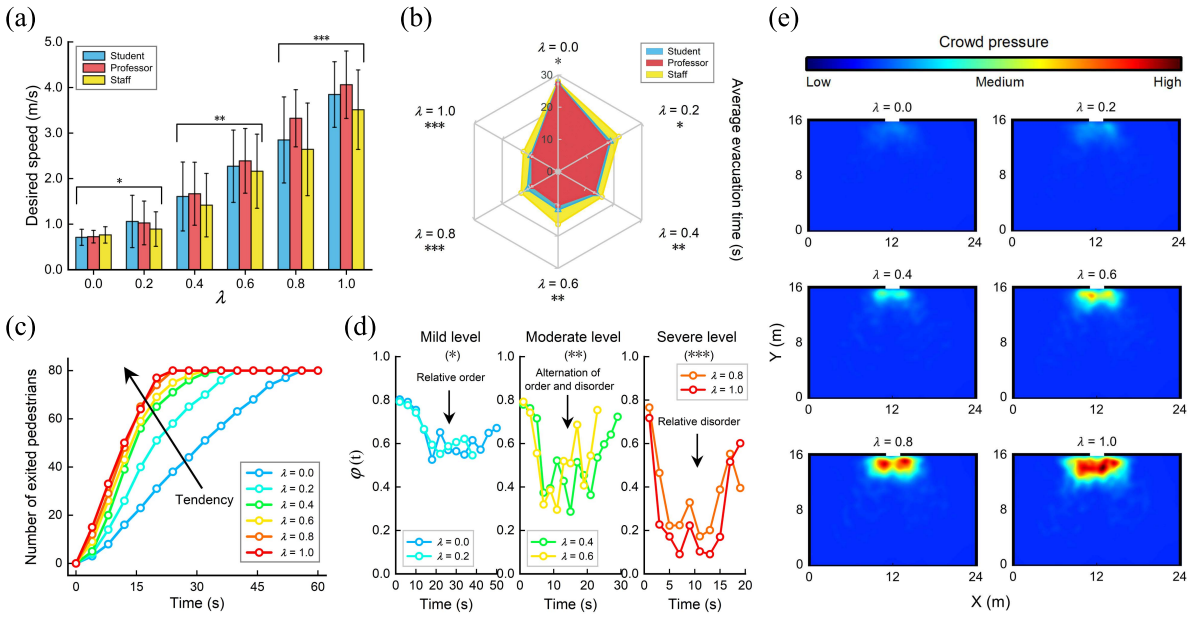

Fig. 5. Influence of risk index on psychology attributes. (a) Variations of the desired speed for specific crowd under different risk indexes. (b) Radar map of the average evacuation time for specific crowd under different risk indexes. (c) Temporal dynamics of the number of exited pedestrians under the influence of risk index. The dashed arrow indicates the trend of the curves when the risk index grows up. (d) Variations of the order parameter under mild, moderate and severe levels. The transformation of crowd changes from relative order to relative disorder as the risk index increases. (e) Characterization of "crowd pressure" in the scene corresponding to the risk index $\lambda = 0.0, 0.2, 0.4, 0.6, 0.8$ and 1.0. Red areas represent a high risk of falling, indicating potential areas of crowd disaster and casualties.

The interaction scenario of library reading room in Fig. 4(d) is more prone to gather crowds and conducive to highlighting the heterogeneous impact of psychology attributes. At initial moment (t =0 s), the pedestrians distributed in different positions begin to escape towards the exit. Then the crowd gathers at the exit to form an "arch", accompanied by the phenomenon that some individuals push against each other (t =8 s). With a further extension of time (t = 16 s and t = 24 s), the majority of staff members remain behind the team to assist others to escape, which seems intuitively consistent with the social difference of specific crowd. Fig. 4(e) depicts the temporal evolution of the number of pedestrians in three kinds of psychology states, and cooperation and competition are prominent after the crowd gathered. Evidently, the staff has a large proportion of cooperation, revealing the reason why most staff stay behind the crowd. Analogously, the results of 10 trials are employed to analyze the influence of the mentality coefficient. In Fig. 4(f), there is little distinction in the average actual speed during the sprint phase, whereas the average actual speed of staff is lower than that of students and professors during the congestion phase. The relatively slow actual speed directly extends the universal evacuation time of the staff in Fig. 4(g). This indicates that psychology attributes, as unique characteristics of human crowds, play an important role in the evacuation process.

E. Influence of Risk Index on Psychology Attributes

Actually, the cooperation probability of specific crowd is significantly different as the risk index λ changes, which may cause differences in the evacuation process. With the increase of the risk index, as shown in Fig. 5(a), the desired speed of crowds rises. In non-emergency situations ($\lambda = 0.0$), the desired speed is low and almost the same due to the high proportion of cooperation. A higher risk index corresponds to a larger distinction of desired speed. This is attributed to the fact that the change in the proportion of cooperation and competition for specific crowd. From Fig. 5(b), for moderate and severe levels of emergencies, professors with lower cooperation probability correspond to the shortest average evacuation time, while the staff with more cooperative behaviors perform the longest average evacuation time due to the professional spirit.

From the perspective of all pedestrians, the temporal dynamics of the number of exited pedestrians are shown in Fig. 5(c). The slope increment of the curve reflects the degree of psychology stimulation in response to a higher risk index, resulting in a higher escape efficiency of total pedestrians. Fig. 5(d) illustrates the variations of order parameter under mild, moderate and severe levels. As the degree of emergency exacerbates, the order parameter curves elucidate the transition of the crowd changes from relatively order to relatively disorder, which is a dangerous phenomenon that may interfere with pedestrian decisions. Furthermore, the curves of evacuation efficiency merely indicate the characteristics from the time dimension, but we expect to conduct a deeper analysis from the spatial dimension. Here, given the "crowd pressure" $C(\mathbf{x})$ [17] to measure the local pressure at place $\mathbf{x}$ as follows:

$$C(\mathbf{x}) = \rho(\mathbf{x}) \, Var_{\mathbf{x}}[V(\mathbf{x}, t)] \tag{18}$$

where $\rho(\mathbf{x}) = \langle \rho(\mathbf{x}, t) \rangle_t$ represents the temporal average of the local density, and the local density at place $\mathbf{x}$ and time t

is measured as follows:

$$\rho\left(\mathbf{x},t\right)=\sum\nolimits_{i} f\left(d_{i\mathbf{x}},t\right) \tag{19}$$

Here, $f\left(d_{i\mathbf{x}}\right)$ is a Gaussian distance-dependent weight function between the position of pedestrian i and place $\mathbf{x}$:

$$f\left(d_{i\mathbf{x}}\right)=\frac{1}{\pi R^{2}}\exp\left(-\frac{d_{i\mathbf{x}}^{2}}{R^{2}}\right) \tag{20}$$

where $R=0.7m$ is a measurement parameter. Besides, $V\left(\mathbf{x},t\right)$ denotes the local speed at place $\mathbf{x}$ and time t by:

$$V\left(\mathbf{x},t\right)=\frac{\sum_{i}\left\|\mathbf{v}_{i}\right\| f\left(d_{i\mathbf{x}},t\right)}{\sum_{i} f\left(d_{i\mathbf{x}},t\right)} \tag{21}$$

Fig. 5(e) characterizes the "crowd pressure" in the scene when $\lambda=0.0, 0.2, 0.4, 0.6, 0.8$ and 1.0. The frequent pushing phenomenon near the exit is caused by the unbalanced distribution of "crowd pressure". Note that the "crowd pressure" at some places (in red) will be extremely large when the risk index is excessive ($\lambda \geq 0.8$), which may lead to the crowd disaster and casualties. In summary, although a higher risk index promotes the evacuation efficiency to a certain extent, it greatly increases the probability of accidents.

F. Comparison of PHSFM With Existing Models

In recent years, some modifications to the SFM have incorporated the factors of pedestrian heterogeneity. Moussaïd *et al.* discovered the desired speed of the crowd follows a Gaussian distribution with the mean $\bar{v}^{0}=1.29\ ms^{-1}$ and the standard deviation $\theta=0.19\ ms^{-1}$, which depends on the physiology factors such as gender and age [40]. Helbing *et al.* adopted the panic parameter to describe the psychology features [13] of pedestrians. The desired speed varying from initial value $v_{i}^{0}=1\ ms^{-1}$ to maximum value $v_{i}^{\max}=2\ ms^{-1}$ is affected by the panic psychology. The above-mentioned models are called as "GSFM" and "PSFM" in this paper, which adjust the desired speed from the physiology and psychology levels to adapt to more realistic situations. In the follow-up phase of the study, the PHSFM is compared with these models to verify its generality.

The optimal parameter estimations corresponding to the above models are generated in PHSFM, where the PHSFM_1 only considers the physique coefficient ($\alpha=\beta=5.15$, $\mu=0.59$ and $\sigma=1.2$) and the PHSFM_2 merely involves the mentality coefficient ($\delta_{i}^{nor}=1$, $\delta_{i}^{max}=2$ and $\Delta_{M}=0$). They are applied to compare with the evacuation process simulated by GSFM and PSFM in the library interaction scenarios, respectively. Fig. 6(a) and 6(b) show the average actual speed of all pedestrians simulated by the above models after 10 trials. Note that the curves of PHSFM_1 and GSFM are nearly consistent, and similar results are also obtained from the simulation of PHSFM_2 and PSFM. For the evacuation time of each pedestrian, the comparison results are illustrated in Fig. 6(c) and 6(d). Simulation data close to the standard line indicate the evacuation time simulated by these models is almost consistent, with the correlations of 0.97 and 0.99. This demonstrates that GSFM and PSFM can be regarded as two special cases of PHSFM.

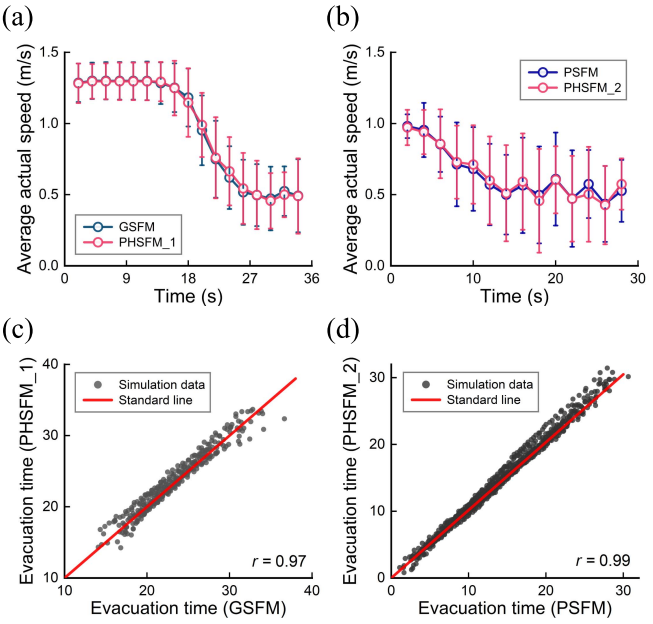

Fig. 6. Comparison of PHSFM with existing models. (a)-(b) Average actual speed of all pedestrians simulated by GSFM and PHSFM_1, PSFM and PHSFM_2 in 10 trials. The shape points on the lines denote the mean value and the error bars represent the standard deviation. (c)-(d) Correlation of evacuation time simulated by GSFM and PHSFM_1, PSFM and PHSFM_2 in 10 trials. The simulation data in standard lines (in red) correspond to the completely consistent results.

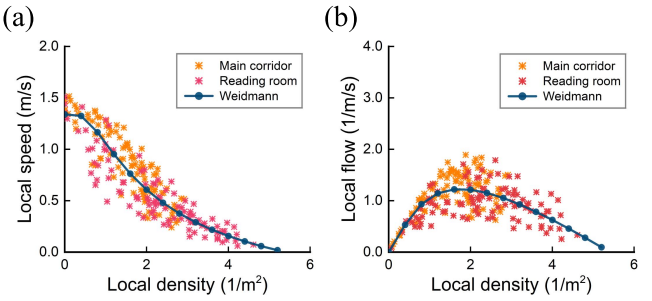

Fig. 7. Fundamental diagrams in the two simulation scenarios simulated by PHSFM. (a) Relationship between local density and speed. (b) Relationship between local density and flow. Our data points from the main corridor and reading room are shown as orange and red stars, and the blue solid curves are from Weidmann [44] as the criterion.

In a word, analogous evacuation processes simulated by GSFM and PSFM can be generated in PHSFM by setting suitable parameters. It implies that the PHSFM provides a general framework for the expression of pedestrian heterogeneity. For example, the initial distribution curves of different shapes can be obtained by adjusting the parameters in physique coefficient, which is of great significance to the simulation for specific crowd. Besides, the psychology states of stress, cooperation and competition are included in mentality coefficient, permitting more elaborate psychology expressions in crowds.

G. Validation Process of PHSFM

As far as the functionality of the model is concerned, the PHSFM successfully simulates the physiology and

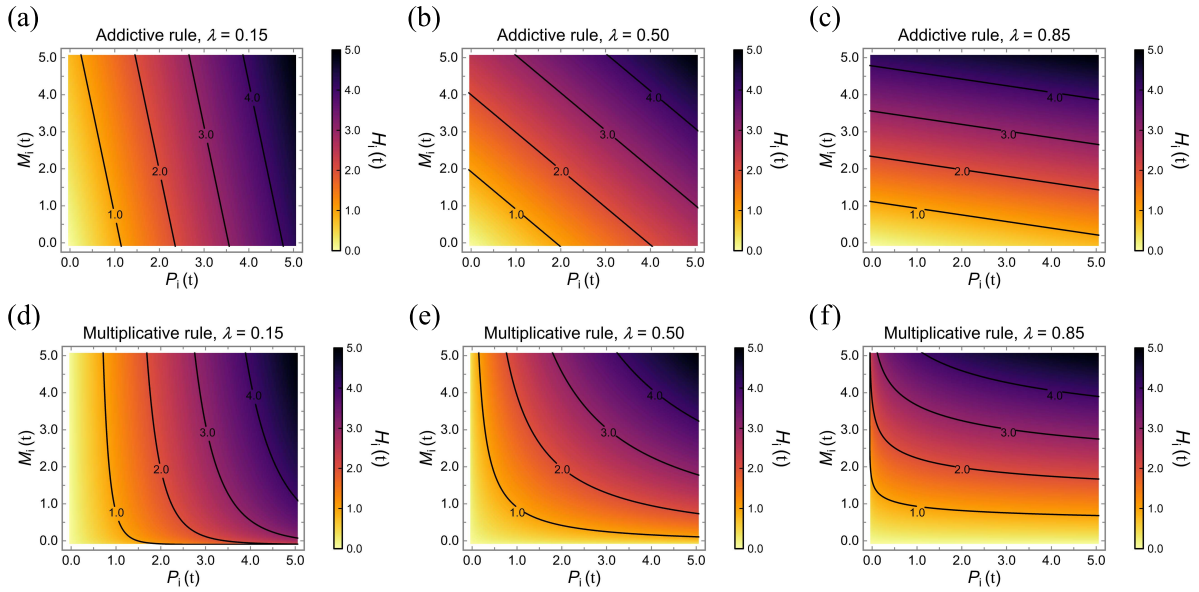

Fig. 8. Contour diagrams of heterogeneous coefficient under different combination rules and risk indexes. (a) Addictive rule, $\lambda = 0.15$. (b) Addictive rule, $\lambda = 0.50$. (c) Addictive rule, $\lambda = 0.85$. (d) Multiplicative rule, $\lambda = 0.15$. (e) Multiplicative rule, $\lambda = 0.50$. (f) Multiplicative rule, $\lambda = 0.85$. In the vertical direction, $\lambda = 0.15$, $\lambda = 0.50$ and $\lambda = 0.85$ represent mild, moderate and severe levels. In the horizontal direction, the additive and multiplicative rules are adopted to combine these coefficients. Different contour lines correspond to different values of heterogeneous coefficient.

psychology heterogeneity of pedestrians, and has stronger scalability than existing models. However, it is necessary to further evaluate whether the model is suitable for describing pedestrian movements. The fundamental diagram [41], [42] is a robust quantitative method used to validate the response of crowd dynamics models by generating the relationships between density and speed, and between density and flow. In our case, the local flow $Q(\mathbf{x}, t)$ is determined according to the fluid-dynamic formula:

$$Q(\mathbf{x}, t) = \rho(\mathbf{x}, t) V(\mathbf{x}, t) \tag{22}$$

where the local density $\rho(\mathbf{x}, t)$ and the local speed $V(\mathbf{x}, t)$ respectively correspond to Equation (19) and (21), details of the above definitions are consulted in [43].

In light of the two simulation scenarios that have been adopted, Fig. 7 shows the corresponding fundamental diagrams by setting appropriate parameters in PHSFM. Here, a most frequently cited fundamental diagram is used as the criterion, the relationship between local density and speed was obtained by collecting and fitting 25 different survey data according to Weidmann [44]:

$$v(\rho) = v_0^{free} \left\{ 1 - \exp\left[-\zeta \left(\frac{1}{\rho} - \frac{1}{\rho_{\max}} \right) \right] \right\} \tag{23}$$

where $v_0^{free} = 1.34\ ms^{-1}$ is the free speed at low densities, the maximal pedestrian density is $\rho_{\max} = 5.4m^{-2}$, and $\zeta = 1.913m^{-2}$ denotes a fit parameter. The blue solid curves in Fig. 7(a) and 7(b) are from Equation (23). The difference in data between the main corridor (orange stars) and reading room (red stars) implies the fundamental diagrams vary by different facilities, since the reading room is more prone to congestion, resulting in greater local density. Despite of this, the fundamental diagrams in the two simulation scenarios simulated by PHSFM are primarily consistent with Weidmann's results, indicating the effectiveness of our model.

H. Extended Analysis of PHSFM

The physiology and psychology factors often jointly determine the pedestrian heterogeneity in real life. How to effectively combine these coefficients has become an important issue. Relevant researches have found the emergency is a huge pressure source for pedestrians, and their endocrine and stress responses in emergencies are significantly different from that in normal conditions [45]. That is to say, the role of psychology attributes becomes increasingly prominent as the risk index λ increases, which might be used as a bond to combine the two coefficients.

Under the premise of ignoring the internal coupling, additive and multiplicative rules are two different mechanisms for combining coefficients or signals, widely used in neurocognition [46], signal processing [47] and other fields. When the additive rule is used to express the function relation $\circ$, given that the risk index λ can be regarded as a weight. The heterogeneous coefficient $H_i(t)$ is defined as a linear combination of $P_i(t)$ and $M_i(t)$:

$$H_i(t) = (1 - \lambda) P_i(t) + \lambda M_i(t) \tag{24}$$

Besides, the multiplicative rule is generally applied to describe the nonlinear variation and form a scaling correlation between these coefficients. Thereby, the expression of heterogeneous coefficient $H_i(t)$ based on function relation $\circ$ is given by:

$$H_i(t) = P_i(t)^{(1-\lambda)} \times M_i(t)^{\lambda} \tag{25}$$

We compare the mentioned methods of combining these coefficients, the contour diagrams of heterogeneous coefficient under different risk indexes are established in Fig. 8. In the horizontal direction, the results obtained by the two combination methods are consistent. For $\lambda = 0.15$ in mild level, the physique coefficient has a greater impact on heterogeneous coefficient. On the contrary, the domination of mentality coefficient is observed for $\lambda = 0.85$ in severe level. With regard to $\lambda = 0.50$ in moderate level, it corresponds to the critical state where both possess the same influence. In the vertical direction, the contour lines in maps indicate the heterogeneous coefficient mainly changes in a linear relationship by additive rule. However, the multiplicative rule increases the degree of nonlinear variation, resulting in stronger restriction between these coefficients. Therefore, the combinations of these coefficients might be considered as specific paradigms for explicating the behavior heterogeneity of pedestrians.

IV. Discussion and Conclusion

This paper presents the PHSFM, which incorporates the pedestrian heterogeneity into the SFM. Different from traditional methods in modeling crowd motion, the quantitative description of pedestrian heterogeneity in our model is an essential step for modeling diverse crowds as it provides specific coefficients to estimate the level of difference. Specifically, the physique coefficient describes the stability characteristic of physiology attributes, and the mentality coefficient characterizes the dynamic transition of psychology states. The innate character of these two coefficients is to change the desired speed in self-driven force, for the purpose of achieving a more realistic simulation of crowd motion.

By conducting numerical experiments in the library interaction scenarios, several prime and interesting conclusions are summarized as follows: Firstly, we demonstrate how the PHSFM can be regarded as a general framework to describe the pedestrian heterogeneity of physiology and psychology, which explicates the escape behavior in a more detailed way. Secondly, the phenomenon that students appear to "catch up" while professors perform "fall behind" in the corridor indicates larger physique coefficients determine shorter evacuation time to some extent, and most staff stay behind the crowd in the reading room denotes the mentality coefficient effectively measures the psychological state difference for specific crowd. Last but not least, these two coefficients are skillfully linked to the risk index of environments. Experiment results indicate the risk index has a certain impact on both coefficients, but greater on mentality coefficient, because the psychology attributes dominate in emergencies. These conclusions essentially emphasize that pedestrians cannot be simply formulated as homogeneous rigid particles assumed in SFM.

The above conclusions provide effective guidelines for the management of crowds in potential research fields. In architectural science, once an emergency occurs, for those "left behind" pedestrians (i.e. older people, patient, and disabled, etc.), how to design effective building structures to promote their evacuation efficiency deserves in-depth consideration [48]. With regard to transportation, the framework of pedestrian heterogeneity can inspire the expression of heterogeneity involving vehicles and even roads, which is beneficial for controlling complex traffic flows [49]. Besides, in researches of safety science on large-scale crowds [50] (i.e. concert, marathon, and football game, etc.), the risk index incorporated in pedestrian heterogeneity may provide the decision-making schemes for crowd evacuation under different types of emergencies (i.e. fire, explosion, and terrorist attack, etc.). Therefore, understanding the pedestrian heterogeneity is a crucial step toward more reliable managements of crowds in real life.

Although the PHSFM considers the physiology and psychology attributes of pedestrians, it is still a simplified model. Many other clues involving the pedestrian heterogeneity, such as information capture, reaction time and other complicated factors, could alter the expression of our model. How to quantify these factors and improve the generalization ability of PHSFM requires a more exhaustive discussion. In fact, our model can be viewed as a typical paradigm. Once other relevant heterogeneous clues are identified through empirical observations or experimental analysis, it will be easy to incorporate them into these coefficients with mathematical expressions. Thereby, mining these clues reflecting pedestrian heterogeneity is an interesting task due to the fact that the diverse forms of individual expression are consistent with our cognitive customs.

Moreover, the pedestrian heterogeneity may not merely affect the self-driven force. That is to say, these clues are not confined to their own heterogeneous characteristics, but may also be embodied in the interaction behaviors with others. In our daily life, people follow certain behavioral patterns, which are altered with the forms of social interaction [51]. For diverse pedestrians, the reactions influenced by the interaction force of other individuals vary to a large extent, resulting in the transformation of their behaviors and trajectories. From a group perspective, as a link between human beings, social relationships such as kinship or friendship are implicit mechanisms for the group formation phenomena. This may lead to specific movement patterns, but little consideration is given in this field at present. Thus, establishing a pedestrian heterogeneity-based model incorporating interaction behaviors remains a formidable challenge. In summary, despite the PHSFM works well for the expression of low-level behavioral pattern and psychological perception, it is inadequate when elucidating the conception of high-level pedestrian interaction and implied relationship.

To summarize, we have demonstrated here a general methodology where our model highlights the prominence of individual heterogeneity, which echoes in many aspects of the natural science, such as the individual differences in human social learning strategies [52], the heterogeneous topology structure of complex networks [53], and the intra-versus intergroup differences of populations in bioscience [54]. In the future, further enhancing the versatility and accuracy of the model is our target. Furthermore, we also expect that this model will stimulate the generation of more elaborate human motion models, which will provide new insights for the field of crowd dynamics.

REFERENCES

[1] A. Bottinelli, D. T. J. Sumpter, and J. L. Silverberg, "Emergent structural mechanisms for high-density collective motion inspired by human crowds," *Phys. Rev. Lett.*, vol. 117, no. 22, Nov. 2016, Art. no. 228301.

[2] A. A. Ganin, M. Kitsak, D. Marchese, J. M. Keisler, T. Seager, and I. Linkov, "Resilience and efficiency in transportation networks," *Sci. Adv.*, vol. 3, no. 12, Dec. 2017, Art. no. e1701079.

[3] N. Shiwakoti and M. Sarvi, "Enhancing the panic escape of crowd through architectural design," *Transp. Res. C, Emerg. Technol.*, vol. 37, pp. 260–267, Dec. 2013.

[4] N. Bain and D. Bartolo, "Dynamic response and hydrodynamics of polarized crowds," *Science*, vol. 363, no. 6422, pp. 46–49, Jan. 2019.

[5] T. Vicsek and A. Zafeiris, "Collective motion," *Phys. Rep.*, vol. 517, nos. 3–4, pp. 71–140, Aug. 2012.

[6] H. J. Charlesworth and M. S. Turner, "Intrinsically motivated collective motion," *Proc. Nat. Acad. Sci. USA*, vol. 116, no. 31, pp. 15362–15367, Jul. 2019.

[7] L. Zhao *et al.*, "Herd behavior in a complex adaptive system," *Proc. Nat. Acad. Sci. USA*, vol. 108, no. 37, pp. 15058–15063, Aug. 2011.

[8] A. Seyfried, B. Steffen, and T. Lippert, "Basics of modelling the pedestrian flow," *Phys. A, Stat. Mech. Appl.*, vol. 368, no. 1, pp. 232–238, Aug. 2006.

[9] M. Moussaïd, N. Perozo, S. Garnier, D. Helbing, and G. Theraulaz, "The walking behaviour of pedestrian social groups and its impact on crowd dynamics," *PLoS ONE*, vol. 5, no. 4, Apr. 2010, Art. no. e10047.

[10] L. F. Henderson, "The statistics of crowd fluids," *Nature*, vol. 229, no. 5284, pp. 381–383, Feb. 1971.

[11] A. Kulkarni, S. P. Thampi, and M. V. Panchagnula, "Sparse game changers restore collective motion in panicked human crowds," *Phys. Rev. Lett.*, vol. 122, no. 4, Jan. 2019, Art. no. 048002.

[12] D. Helbing and P. Molnár, "Social force model for pedestrian dynamics," *Phys. Rev. E, Stat. Phys. Plasmas Fluids Relat. Interdiscip. Top.*, vol. 51, no. 5, pp. 4282–4286, May 1995.

[13] D. Helbing, I. Farkas, and T. Vicsek, "Simulating dynamical features of escape panic," *Nature*, vol. 407, no. 6803, pp. 487–490, Sep. 2000.

[14] W. Yu and A. Johansson, "Modeling crowd turbulence by many-particle simulations," *Phys. Rev. E, Stat. Phys. Plasmas Fluids Relat. Interdiscip. Top.*, vol. 76, no. 4, Oct. 2007, Art. no. 046105.

[15] X. Chen, M. Treiber, V. Kanagaraj, and H. Li, "Social force models for pedestrian traffic–state of the art," *Transp. Rev.*, vol. 38, no. 5, pp. 625–653, Nov. 2017.

[16] X. Song, H. Xie, J. Sun, D. Han, Y. Cui, and B. Chen, "Simulation of pedestrian rotation dynamics near crowded exits," *IEEE Trans. Intell. Transp. Syst.*, vol. 20, no. 8, pp. 3142–3155, Aug. 2019.

[17] M. Moussaid, D. Helbing, and G. Theraulaz, "How simple rules determine pedestrian behavior and crowd disasters," *Proc. Nat. Acad. Sci. USA*, vol. 108, no. 17, pp. 6884–6888, Apr. 2011.

[18] H. B. Menz, "Age-related differences in walking stability," *Age Ageing*, vol. 32, no. 2, pp. 137–142, Mar. 2003.

[19] J. Drury *et al.*, "Cooperation versus competition in a mass emergency evacuation: A new laboratory simulation and a new theoretical model," *Behav. Res. Methods*, vol. 41, no. 3, pp. 957–970, Aug. 2009.

[20] S. Bouzat and M. N. Kuperman, "Game theory in models of pedestrian room evacuation," *Phys. Rev. E, Stat. Phys. Plasmas Fluids Relat. Interdiscip. Top.*, vol. 89, no. 3, Mar. 2014, Art. no. 032806.

[21] A. Templeton, J. Drury, and A. Philippides, "From mindless masses to small groups: Conceptualizing collective behavior in crowd modeling," *Rev. Gen. Psychol.*, vol. 19, no. 3, pp. 215–229, Sep. 2015.

[22] X. Guo, J. Chen, Y. Zheng, and J. Wei, "A heterogeneous lattice gas model for simulating pedestrian evacuation," *Phys. A, Stat. Mech. Appl.*, vol. 391, no. 3, pp. 582–592, Feb. 2012.

[23] Y. Li, M. Chen, X. Zheng, Z. Dou, and Y. Cheng, "Relationship between behavior aggressiveness and pedestrian dynamics using behavior-based cellular automata model," *Appl. Math. Comput.*, vol. 371, Apr. 2020, Art. no. 124941.

[24] D. Guo, C. Wang, and X. Wang, "A hierarchical pedestrians motion planning model for heterogeneous crowds simulation," in *Proc. Int. Conf. Inf. Automat.*, Jun. 2009, pp. 1363–1367.

[25] Q. Liu, "The effect of dedicated exit on the evacuation of heterogeneous pedestrians," *Phys. A, Stat. Mech. Appl.*, vol. 506, pp. 305–323, Sep. 2018.

[26] D. S. Stuart, M. S. Sharifi, K. M. Christensen, A. Chen, Y. S. Kim, and Y. Chen, "Crowds involving individuals with disabilities: Modeling heterogeneity using fractional order potential fields and the social force model," *Phys. A, Stat. Mech. Appl.*, vol. 514, pp. 244–258, Jan. 2019.

[27] C. Caramuta, G. Collodel, C. Giacomini, C. Gruden, G. Longo, and P. Piccolotto, "Survey of detection techniques, mathematical models and simulation software in pedestrian dynamics," *Transp. Res. Procedia*, vol. 25, pp. 551–567, Jan. 2017.

[28] M. H. Zaki and T. Sayed, "Using automated walking gait analysis for the identification of pedestrian attributes," *Transp. Res. C, Emerg. Technol.*, vol. 48, pp. 16–36, Nov. 2014.

[29] S. Yachi and M. Loreau, "Biodiversity and ecosystem productivity in a fluctuating environment: The insurance hypothesis," *Proc. Nat. Acad. Sci. USA*, vol. 96, no. 4, pp. 1463–1468, Feb. 1999.

[30] J. M. Hausdorff, "Gait dynamics, fractals and falls: Finding meaning in the stride-to-stride fluctuations of human walking," *Hum. Movement Sci.*, vol. 26, no. 4, pp. 555–589, Aug. 2007.

[31] F. Ozel, "Time pressure and stress as a factor during emergency egress," *Saf. Sci.*, vol. 38, no. 2, pp. 95–107, Jul. 2001.

[32] C. L. Bethel and R. R. Murphy, "Survey of non-facial/non-verbal affective expressions for appearance-constrained robots," *IEEE Trans. Syst., Man, Cybern. C, Appl. Rev.*, vol. 38, no. 1, pp. 83–92, Jan. 2008.

[33] F. Garrido-Charad *et al.*, "'Shepherd's crook' neurons drive and synchronize the enhancing and suppressive mechanisms of the midbrain stimulus selection network," *Proc. Nat. Acad. Sci. USA*, vol. 115, no. 32, pp. E7615–E7623, Jul. 2018.

[34] Y. Cheng and X. Zheng, "Effect of uncertainty on cooperative behaviors during an emergency evacuation," *Commun. Nonlinear Sci. Numer. Simul.*, vol. 66, pp. 216–225, Jan. 2019.

[35] C. A. Hill, S. Suzuki, R. Polania, M. Moisa, J. P. O'Doherty, and C. C. Ruff, "A causal account of the brain network computations underlying strategic social behavior," *Nature Neurosci.*, vol. 20, no. 8, pp. 1142–1149, Jul. 2017.

[36] S. Xu and H. B.-L. Duh, "A simulation of bonding effects and their impacts on pedestrian dynamics," *IEEE Trans. Intell. Transp. Syst.*, vol. 11, no. 1, pp. 153–161, Mar. 2010.

[37] B. Allen, B. Curless, and Z. Popović, "The space of human body shapes," *ACM Trans. Graph.*, vol. 22, no. 3, p. 587, Jul. 2003.

[38] T. Vicsek, A. Czirók, E. Ben-Jacob, I. Cohen, and O. Shochet, "Novel type of phase transition in a system of self-driven particles," *Phys. Rev. Lett.*, vol. 75, no. 6, pp. 1226–1229, Aug. 1995.

[39] A. C. Jenkins, P. Karashchuk, L. Zhu, and M. Hsu, "Predicting human behavior toward members of different social groups," *Proc. Nat. Acad. Sci. USA*, vol. 115, no. 39, pp. 9696–9701, Sep. 2018.

[40] M. Moussaïd, D. Helbing, S. Garnier, A. Johansson, M. Combe, and G. Theraulaz, "Experimental study of the behavioural mechanisms underlying self-organization in human crowds," *Proc. Roy. Soc. B, Biol. Sci.*, vol. 276, no. 1668, pp. 2755–2762, May 2009.

[41] A. Seyfried, B. Steffen, W. Klingsch, and M. Boltes, "The fundamental diagram of pedestrian movement revisited," *J. Stat. Mech., Theory Exp.*, vol. 2005, no. 10, p. P10002, Oct. 2005.

[42] A. Tsiftsis, I. G. Georgoudas, and G. C. Sirakoulis, "Real data evaluation of a crowd supervising system for stadium evacuation and its hardware implementation," *IEEE Syst. J.*, vol. 10, no. 2, pp. 649–660, Jun. 2016.

[43] D. Helbing, A. Johansson, and H. Z. Al-Abideen, "Dynamics of crowd disasters: An empirical study," *Phys. Rev. E, Stat. Phys. Plasmas Fluids Relat. Interdiscip. Top.*, vol. 75, no. 4, Apr. 2007.

[44] U. Weidmann, "Transporttechnik der fussgänger," in *Transporttechnische Eigenschaften des Fussgängerverkehrs* (Schriftenreihe des IVT Nr. 90), 2nd ed. Zurich, Switzerland: ETH Zürich, Mar. 1993.

[45] A. Keitel *et al.*, "Endocrine and psychological stress responses in a simulated emergency situation," *Psychoneuroendocrinology*, vol. 36, no. 1, pp. 98–108, Jan. 2011.

[46] N. A. R. Murty and S. P. Arun, "Multiplicative mixing of object identity and image attributes in single inferior temporal neurons," *Proc. Nat. Acad. Sci. USA*, vol. 115, no. 14, pp. E3276–E3285, Mar. 2018.

[47] P. P. Mitra and J. B. Stark, "Nonlinear limits to the information capacity of optical fibre communications," *Nature*, vol. 411, no. 6841, pp. 1027–1030, Jun. 2001.

[48] J. Koo, Y. S. Kim, B.-I. Kim, and K. M. Christensen, "A comparative study of evacuation strategies for people with disabilities in high-rise building evacuation," *Expert Syst. Appl.*, vol. 40, no. 2, pp. 408–417, Feb. 2013.

[49] Y. Ren, M. Ercsey-Ravasz, P. Wang, M. C. González, and Z. Toroczkai, "Predicting commuter flows in spatial networks using a radiation model based on temporal ranges," *Nature Commun.*, vol. 5, no. 1, p. 5347, Nov. 2014.

[50] J. L. Silverberg, M. Bierbaum, J. P. Sethna, and I. Cohen, "Collective motion of humans in mosh and circle pits at heavy metal concerts," *Phys. Rev. Lett.*, vol. 110, no. 22, May 2013, Art. no. 228701.

[51] C. Zhou, M. Han, Q. Liang, Y.-F. Hu, and S.-G. Kuai, "A social interaction field model accurately identifies static and dynamic social groupings," *Nature Hum. Behav.*, vol. 3, no. 8, pp. 847–855, Jun. 2019.
[52] L. Molleman, P. van den Berg, and F. J. Weissing, "Consistent individual differences in human social learning strategies," *Nature Commun.*, vol. 5, no. 1, p. 3570, Apr. 2014.
[53] S. Wang *et al.*, "Inferring dynamic topology for decoding spatiotemporal structures in complex heterogeneous networks," *Proc. Nat. Acad. Sci. USA*, vol. 115, no. 37, pp. 9300–9305, Aug. 2018.
[54] D. Knebel, A. Ayali, M. Guershon, and G. Ariel, "Intra- versus inter-group variance in collective behavior," *Sci. Adv.*, vol. 5, no. 1, Jan. 2019, Art. no. eaav0695.

Wenhan Wu received the B.S. degree from the School of Automation, Central South University, Changsha, China, in 2019. He is currently pursuing the Ph.D. degree in control science and engineering with the Tsinghua University, Beijing, China. His current research interests include crowd dynamics, collective behavior, emergency evacuation, and swarm intelligent robot.

Maoyin Chen (Member, IEEE) received the B.S. degree in mathematics and the M.S. degree in control theory and control engineering from Qufu Normal University, Shandong, China, in 1997 and 2000, respectively, and the Ph.D. degree in control theory and control engineering from Shanghai Jiao Tong University, Shanghai, China, in 2003.

From 2003 to 2005, he was a Post-Doctoral Researcher with the Department of Automation, Tsinghua University, Beijing, China. From 2006 to 2008, he visited University of Potsdam, Potsdam, Germany, as an Alexander von Humboldt Research Fellow. Since October 2008, he has been an Associate Professor with the Department of Automation, Tsinghua University. He has authored or coauthored over 100 peer-reviewed international journal articles. His research interests include fault prognosis and complex systems. He has won the First Prize in natural science (2011, ranked first) and the Second Prize (2019, ranked first) of CAA.

Jinghai Li received the B.S. degree in automation and the M.S. degree in control science and engineering from Tianjin University, Tianjin, China, in 2009 and 2016, respectively. He is currently pursuing the Ph.D. degree in control science and engineering with Tsinghua University, Beijing, China. His current research interests include crowd dynamics, planning and control of robotic systems, and adaptive systems.

Binglu Liu received the B.S. degree from the Department of Automation and the M.S. degree in control science and engineering from Tsinghua University, Beijing, China, in 2017 and 2020, respectively. Her current research interests include crowd dynamics, emergency evacuation, and visual interactive networks.

Xiaoping Zheng received the B.S. degree from the Chengdu University of TCM, Chengdu, China, in 1995, and the Ph.D. degree from Sichuan University, Chengdu, in 2003.

From 2004 to 2006, he was a Post-Doctoral Researcher with the School of Management, Fudan University, Shanghai, China. From 2006 to 2013, he was a Professor with the Institute of Safety Management, Beijing University of Chemical Technology, Beijing, China. He is currently a Professor with the Department of Automation, Tsinghua University, Beijing. His current research interests include large-scale crowd evacuation, evolutionary game theory, and terahertz technology. He was a 973 Chief Scientist in 2011 and a recipient of the National Science Fund for Distinguished Young Scholars in 2012.